



Supplement of

InnFLUX – an open-source code for conventional and disjunct eddy covariance analysis of trace gas measurements: an urban test case

Marcus Striednig et al.

Correspondence to: Thomas Karl (thomas.karl@uibk.ac.at)

The copyright of individual parts of the supplement might differ from the CC BY 4.0 License.

Supplementary material to:

innFLUX - An open source code for conventional and disjunct eddy covariance analysis of trace gas measurements: An urban test case

Marcus Striednig^{1,2}, Martin Graus¹, Thomas G. Karl¹

5 ¹ACINN (Institute of Atmospheric and Cryospheric Science) Leopold-Franzens University Innsbruck, Austria
Institute for Ion- and Applied Physics, Leopold-Franzens University Innsbruck, Austria

Correspondence to: Thomas Karl (thomas.karl@uibk.ac.at)

Content

S.1 Flow Chart

10

S.2 Comparison with Eddy Pro

S.3 Calibration setup used for the PTR-QiTof-MS

15 **S.4 Spectral Analysis and Corrections**

S.5 Supplementary References

S.1 Flow Chart

The workflow of the innFLUX code is illustrated in Figure S1, which depicts a flow chart of the individual processing steps. The sequence of steps needing user input or feedback starts with the first step (step 0), which is only necessary when the directional planar fit option is used for anemometer tilt correction. Step 0 is followed by step 1 and 2. Steps 0, 1 and 2 correspond to the MATLAB scripts innFLUX_step0, innFLUX_step1 and innFLUX_step2, respectively. Input, intermediary and result output files are displayed in orange, and manual steps to be performed by the user are displayed in blue.

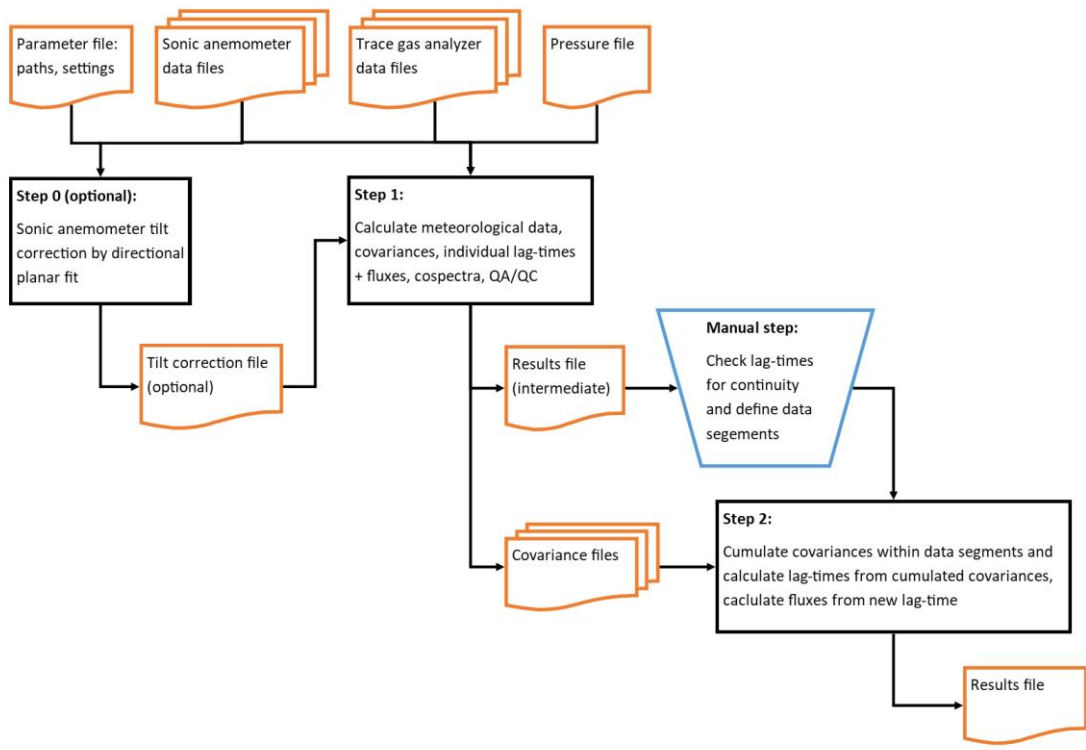


Figure S1: Flow chart showing the processing steps and data flow of innFLUX.

S.2 Comparison with EddyPro®

We performed a comparison between flux results obtained by the innFLUX code and EddyPro. Performing a rigorous comparison of various eddy covariance software packages can be a complex task, as pointed out by Fratini and Mauder (2014) in their in-depth comparison of EddyPro and TK3. While such a detailed comparison would be out of the scope of the present publication, we show some basic evaluations between innFLUX and EddyPro. To perform a meaningful comparison

we choose available parameters in EddyPro in a way to match the parameters used for innFLUX as closely as possible. For anemometer tilt correction, we used the double rotation method, because it should be implemented the same way in EddyPro as in innFLUX. We did not apply any automatic spectral corrections. Results were filtered for high quality fluxes, using only fluxes of quality class 3 or below on the 1-9 scale introduced by Foken et al., 2004. Figure S2 shows a scatter plot of the 5 CO₂ flux calculated by innFLUX against the flux calculated by EddyPro. Figure S3 shows a corresponding plot for the sensible heat flux. Overall innFLUX and EddyPro compare well with a slope of 1.02 (0.95) and an r^2 of 0.97 (0.99) for CO₂ (sensible heat) fluxes.

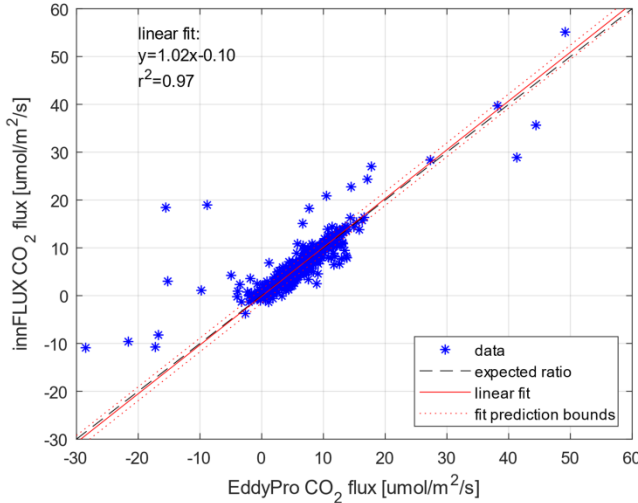


Figure S2: Scatter plot of CO₂ fluxes calculated by innFLUX, and plotted against fluxes calculated by EddyPro.

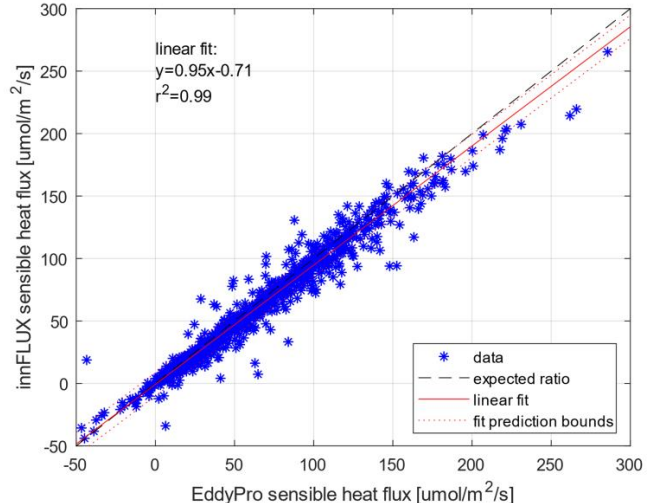


Figure S3: Scatter plot of sensible heat fluxes calculated by innFLUX, and plotted against fluxes calculated by EddyPro.

10

S.3 Calibration setup used for the PTR-QiTof-MS

The PTR-QiTof-MS was calibrated using a calibration gas standard CC447665 from Apel-Riemer Environmental, Inc. The standard was used for sensitivity calibrations of the PTR-QiTof-MS. The standard contained mixing ratios of individual compounds between 1 and 5 ppmv. The uncertainty of mixing ratios of the pure compounds was taken as 5%. A continuous, 15 controlled flow (Bronkhorst Mass Flowcontroller F-200CV-002, 5 sccm, Kalrez plunger) was dynamically diluted into VOC free air (catalytically scrubbed, Parker Zero Air Generator, model 1001) to produce calibration mixtures in the low double digit ppbv range. Table S1 lists the compounds of the calibration gas used in this study.

Table S1: Compounds of the calibration gas used to quantify VOC concentrations measured by the PTR-QiTOF-MS.

| compound | protonated parent ion | m/z |
|----------------------------|--|-----------|
| Methanol | (CH ₄ O)H ⁺ | 33.03350 |
| Acetonitrile | (C ₂ H ₃ N)H ⁺ | 42.03382 |
| Acetaldehyde | (C ₂ H ₄ O)H ⁺ | 45.03350 |
| Acetone | (C ₃ H ₆ O)H ⁺ | 59.04914 |
| DMS | (C ₂ H ₆ S)H ⁺ | 63.02629 |
| Methyl-Ethyl-Ketone | (C ₄ H ₈ O)H ⁺ | 73.06480 |
| Benzene | (C ₆ H ₆)H ⁺ | 79.05422 |
| 2-Methyl-3-buten-2-ol | (C ₅ H ₁₀ O)H ⁺ | 87.08045 |
| Toluene | (C ₇ H ₈)H ⁺ | 93.06988 |
| m-Xylene | (C ₈ H ₁₀)H ⁺ | 107.08553 |
| 1,3,5-Trimethylbenzene | (C ₉ H ₁₂)H ⁺ | 121.10118 |
| 1,2,4,5-Tetramethylbenzene | (C ₁₀ H ₁₄)H ⁺ | 135.11683 |
| alpha-Pinene | (C ₁₀ H ₁₆)H ⁺ | 137.13248 |

S.4 Spectral Analysis and Corrections

Co-spectra of scalars and vertical wind speed are a standard output of innFLUX and are calculated by means of fast Fourier transform (FFT). Co-spectra normalized by the integral over the entire frequency range (equals the covariance), frequency scaled and bin-averaged into 60 log-spaced intervals over 6 decades of non-dimensional frequency

$$\eta = f \cdot (z_m - d) / \bar{u} \quad (\text{S4.1})$$

are stored for each 30-minute period. Only co-spectra of half-hour periods were considered for that spectral analysis that a) pass at a quality class (Foken et al. 2012b) of three or less, b) pass the u^* filtering and c) show a flux signal-to-noise ratio (SNR) of three or more to exclude spectra from periods where the covariance is very noisy. These scaled, non-dimensional co-spectra can be averaged for each scalar (e.g. for toluene measured by PTR-Qi-TOF at 93.06988 m/z). An analytical function

$$fCo(\eta) = A_0 \cdot \frac{\eta / \eta_x}{[1 + m \cdot (\eta / \eta_x)^2 \mu]^{1/(m+1)}}, m \equiv 3/4 \quad (\text{S4.2})$$

(see Lee et al. 2010 and references therein) was fitted to the mean co-spectrum to define a model spectrum for each scalar. Figure S4 shows the mean cospectrum of toluene (open circles) and the fitted model cospectrum (red). Fitting the model cospectrum was weighted strongly towards a two decade wide window around the cospectral maximum (black line in Figure S4).

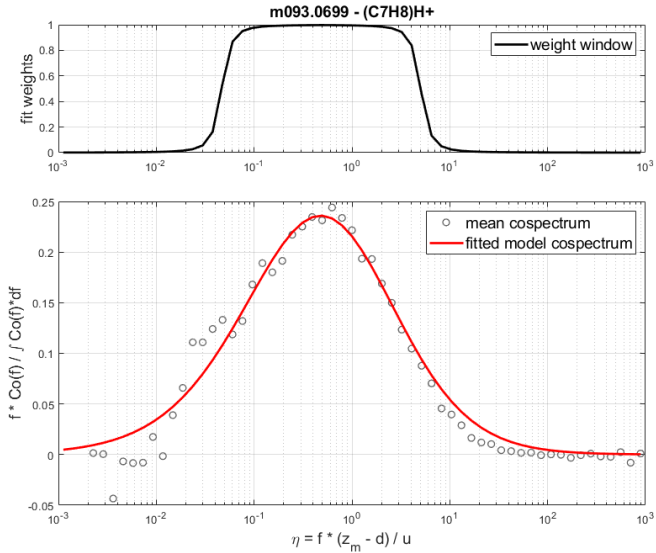


Figure S4. Model spectrum (red line) in Equ. S4.2 was fitted to the average of normalized, frequency scaled toluene cospectra that passed quality checks a-c (N=800) (open circles). The fit was weighted around the cospectral maximum (black line).

5 For each half hour, a model spectrum $Co(f, \bar{u})$ is derived from the non-dimensional model spectrum in dimensional frequency based on the mean wind speed and the measurement height above the displacement plane (see red line in bottom panel of Figure 7 in the main text).

Transfer functions (see top panel of Figure 7 in the main text) for sensor separation, path averaging of the sonic anemometer, path averaging in PTR-MS drift tube, and gas inlet tube attenuation were calculated for each half-hour as described by Foken

10 et al. (2012b) and the references therein and listed here.

Sensor Separation: High frequency attenuation due to lateral separation of the sonic anemometer and the intake of the gas sample inlet manifold can be described by the transfer function

$$T_{ss}(f, \bar{u}, \beta_{WD}) = e^{-9.9 \cdot \left(\frac{f \cdot d_{sa} \cdot |\sin(\beta_{WD} - \beta_{sa})|}{\bar{u}} \right)^{1.5}} \quad (S4.3)$$

where f is the frequency, \bar{u} and β_{WD} are mean horizontal wind speed and direction of the respective averaging period. The 15 geometry parameters d_{sa} and β_{sa} describe length and angle of the vector pointing from the intake to the center of the sonic paths.

Sonic Path Averaging: The path averaging of the wind sonic anemometer is taken care of by the approximation

$$T_{pw}(f, \bar{u}) = \frac{2}{\pi \cdot \eta_w} \left(1 + \frac{e^{-2\pi \cdot \eta_w}}{2} - 3 \frac{1 - e^{-2\pi \cdot \eta_w}}{4\pi \cdot \eta_w} \right) \text{ with } \eta_w = \frac{f \cdot d_{pl}}{\bar{u}} \quad (S4.4)$$

where d_{pl} is the sonic anemometer path length (geometry parameter).

20 **Sensor Path Averaging:** The averaging along the primary ion path as they traverse the drift tube of the PTR-Qi-TOF is represented by

$$T_{ps}(f) = \frac{1}{2\pi\cdot\eta_s} \left(3 + e^{-2\pi\cdot\eta_s} - 4 \frac{1-e^{-2\pi\cdot\eta_s}}{2\pi\cdot\eta_s} \right) \text{ with } \eta_s = \frac{f\cdot d_s}{v_{sample}} \quad (\text{S4.5})$$

with d_s being the length of the drift tube and v_{sample} the flow velocity of the sample gas (not the ions!) along the drift tube. Note that v_{sample} depends on the gas flow rate through the drift tube, drift pressure and temperature and the cross section area and therefore needs to be determined for the specific geometry and settings parameters of the respective PTR-MS instrument. Essentially, d_s over v_{sample} is the characteristic exchange time of the drift tube gas volume.

Tube attenuation: If the tube flow is turbulent, the tube attenuation is described by

$$T_{ta}(f) = \exp \left(-160 \cdot Re^{-1/8} \cdot \frac{\pi^2 \cdot r_t^5 \cdot f^2 \cdot L_t}{Q^2} \right) \quad (\text{S4.6})$$

with the geometry parameters r_t and L_t being inner tube radius and tube length, Q being the volumetric tube flow, and Re being the Reynold's number, which is a function of Q , r_t and kinetic viscosity of the sample air. Note that one needs to make sure that Q is constant and/or measured. Inlet sections with different geometries or flows are treated as separate transfer function. For the VOC flux measurement in the presented setup the inlet manifold transporting sample gas from near the anemometer to the laboratory and the subsampling of the PTR-Qi-TOF through a PEEK capillary were treated separately, but Figure 7 shows that the attenuation in the capillary is negligible.

The total transfer function (Figure 7 black dashed line in top panel) for the high frequency attenuation is

$$T_{HF}(f, \bar{u}, \beta_{WD}) = T_{ss}(f, \bar{u}, \beta_{WD}) \cdot \sqrt{T_{pw}(f, \bar{u})} \cdot \sqrt{T_{ps}(f)} \cdot \sqrt{T_{ta1}(f)} \cdot \sqrt{T_{ta2}(f)} \quad (\text{S4.7})$$

The multiplication of the model co-spectra with the product of the transfer functions results in attenuated co-spectra. The relative error on the flux introduced by high frequency attenuation (low-pass filtering) is given by

$$L_{HF}(\bar{u}, \beta_{WD}) = 1 - \frac{\int_0^{\infty} Co(f, \bar{u}) \cdot T_{HF}(f, \bar{u}, \beta_{WD}) df}{\int_0^{\infty} Co(f, \bar{u}) df} \quad (\text{S4.8})$$

The ratio of the integrals on the right hand side (attenuation) is exemplarily shown in Figure 7 (black dashed line in bottom panel) along with the model spectrum (red line in bottom panel) in a similar way to Foken et al. (2012a). Note that the high frequency loss depends on operational settings, geometry parameters as well as the mean wind speed and direction of each flux averaging period. The measured co-variance of each scalar of each flux averaging period is corrected for the considered high frequency losses by dividing it by the ratio of the integrals in equation S4.8. The mean high frequency loss can be determined from the slope of a linear regression of the uncorrected versus corrected flux (Figure S5).

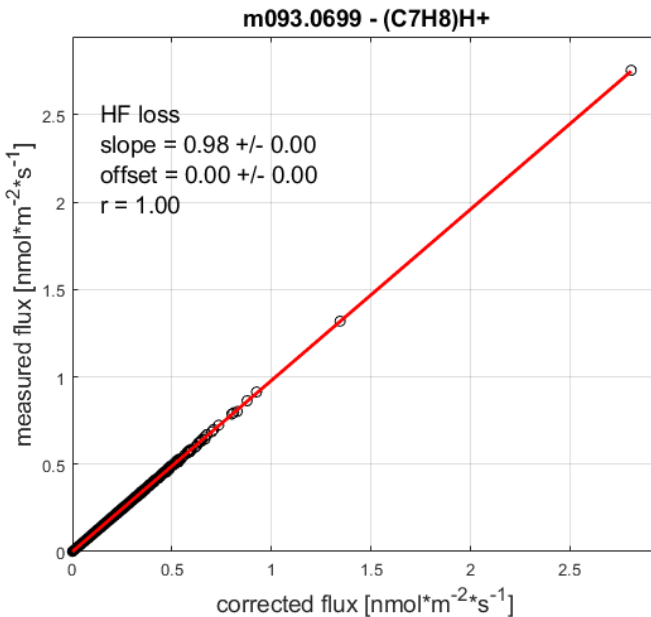


Figure S5. Scatter plot of uncorrected versus corrected fluxes of toluene. The linear regression slope indicates a mean high frequency loss of 2%.

5 The geometry and operational parameters for the PTR-Qi-TOF flux measurement setup is listed in Table S2.

Table S2: transfer functions (TF) for high frequency loss and applied parameters

| HF loss process | parameter values |
|----------------------------|---|
| Sensor separation | $d_{sa} = 0.18 \text{ m}$ $\beta_{sa} = 76^\circ$ |
| Sonic path averaging | $d_{pl} = 0.1 \text{ m} / \sin(60^\circ)$ |
| Drift tube path averaging | $\frac{d_s}{v_{sample}} = 0.08 \text{ s}$ |
| Inlet manifold attenuation | $L_t = 13.2 \text{ m}$ $r_t = 3.175 \cdot 10^{-3} \text{ m (1/4" ID)}$ $Q = 18.9 \cdot 10^{-3} \text{ m}^3 \text{ min}^{-1} \text{ at STP}$ |
| Capillary attenuation | $L_t = 1.6 \text{ m}$ $r_t = 0.5 \cdot 10^{-3} \text{ m}$ $Q = 0.45 \cdot 10^{-3} \text{ m}^3 \text{ min}^{-1} \text{ at STP}$ |

S.5 Supplementary References

Foken, T., Gockede, M., Mauder, M., Mahrt, L., Amiro, B. D., and Munger, J. W.: Post-field quality control, in: *Handbook of Micrometeorology: A Guide to Surface Flux Measurements*, edited by: Lee, X., Massman, W., and Law, B., Springer Science + Business Media, Inc., 67-99, ISBN 978-1-4020-2265-4, <https://doi.org/10.1007/1-4020-2265-4>, 2004.

5

Foken T., Aubinet M., Leuning R.: The Eddy Covariance Method, in: *Eddy Covariance*. Springer Atmospheric Sciences, edited by: Aubinet M., Vesala T., Papale D., Springer, Dordrecht, https://doi.org/10.1007/978-94-007-2351-1_1, 2012a.

Foken, T, Leuning, R., Oncley, S. R., Mauder, M., and Aubinet, M.: Corrections and Data Quality Control, in: *Eddy Covariance: A Practical Guide to Measurement and Data Analysis*, edited by: Aubinet, M., Vesala, T., and Papale, D., Dordrecht: Springer Netherlands, https://doi.org/10.1007/978-94-007-2351-1_4, 2012b.

10

Fratini, G. and Mauder, M.: Towards a consistent eddy-covariance processing: an intercomparison of EddyPro and TK3, *Atmos. Meas. Tech.*, 7, 2273-2281, doi:10.5194/amt-7-2273-2014, 2014.

15

Lee, X., Massman, W.J., and Law, B.E.: *Handbook of Micrometeorology: A Guide for Surface Flux Measurement and Analysis*, Kluwer Academic, http://books.google.com/books?id=IJ_19RkTfBQC, ISBN: 9781402022654, 2004.